

BeppoSAX average spectra of Seyfert galaxies

A. Malizia¹, L. Bassani¹, J. B. Stephen¹ and G. Di Cocco¹

IASF, Via Gobetti 101, 40129 Bologna, Italy

angela.malizia@bo.iasf.cnr.it

F. Fiore²

Osservatorio Astronomico di Roma, Via dell'Osservatorio, I-00044 Monteporzio Catone, Italy

and

A.J.Dean³

Physics Department, University of Southampton, Highfield, Southampton S09-5NH, UK

ABSTRACT

We have studied the average 3-200 keV spectra of Seyfert galaxies of type 1 and 2, using data obtained with BeppoSAX. The average Seyfert 1 spectrum is well-fitted by a power law continuum with photon spectral index $\Gamma \sim 1.9$, a Compton reflection component $R \sim 0.6-1$ (depending on the inclination angle between the line of sight and the reflecting material) and a high-energy cutoff at around 200 keV; there is also an iron line at 6.4 keV characterized by an equivalent width of 120 eV. Seyfert 2's on the other hand show stronger neutral absorption ($N_H = 3-4 \times 10^{22}$ atoms cm $^{-2}$) as expected but are also characterized by an X-ray power law which is substantially harder ($\Gamma \sim 1.75$) and with a cut-off at lower energies ($E_c \sim 130$ keV); the iron line parameters are instead substantially similar to those measured in type 1 objects. There are only two possible solutions to this problem: to assume more reflection in Seyfert 2 galaxies than observed in Seyfert 1 or more complex absorption than estimated in the first instance. The first possibility is ruled out by the Seyfert 2 to Seyfert 1 ratio while the second provides an average Seyfert 2 intrinsic spectrum very similar to that of the Seyfert 1. The extra absorber is likely an artifact due to summing spectra with different amounts of absorption, although we cannot exclude its presence in at least some individual sources. Our result argues strongly for a very similar central engine in both type of galaxies as expected under the unified theory.

Subject headings: active galaxies:Seyfert

1. Introduction

The discovery of broad emission lines in the polarized spectrum of a number of Seyfert (Sey) 2 galaxies has provided the basis for a unified model of Sey galaxies in which the main discriminating parameter is the inclination of our line of sight with respect to an obscuring torus surrounding the source. In the simple version of this model, one then expects the direct continuum of type 1 and 2 objects to be identical except for the effects of obscuration by the torus material. The X-ray spectra of type 1 objects are relatively well known and consist of a power law of index ~ 2 , a cut-off at around 200 keV plus a Compton reflection component with R (the solid angle in units of 2π , subtended by the reflecting material) $\sim 0.6\text{--}1$ and a Fe $K\alpha$ feature (Perola et al. 2002, Matt 2001, Pounds and Reeves 2002). Conversely, the X-ray spectra of type 2 are much less well defined due to the extra complexity of absorption: constraints on individual spectra are rather poor due to the limited photon statistics and provide a greater variety of spectral components (Matt et al. 2000, Malaguti et al. 1999, Turner et al. 2000). One way to better constrain the X-ray spectral properties is to consider average spectra. When this is done, the spectra of type 2 objects are found to be substantially harder than that of type 1, which implies a lower energy cut-off (Zdziarski et al. 1995, 2000). However, this intrinsic difference in the spectrum of Sey 1 and 2's cannot be explained by the simplest version of the unified AGN model, providing its strongest challenge yet. Here, we study the average spectra of Sey 1 and 2 observed by BeppoSAX over the energy band 3-200 keV, i.e. the first simultaneous broad band spectra with coverage above 10 keV. The purpose of this work is to impose the tightest possible constraints on both spectral shapes in order to check if their intrinsic continuum is indeed different and to discuss our findings in the framework of the unified theory.

2. The average spectra

The sample used for this work consists of 9 Sey 1 (Fairall9, 3C120, NGC3783, NGC4593, MCG-6-30-15, NGC5548, MKN509, ESO141-G55, NGC7469) and 13 Sey 2 (NGC526A, NGC2992, NGC5506, ESO103-G35, NGC7172, NGC7314, NGC7582, MCG-5-23-16, NGC1365, NGC2110, NGC4258, NGC5252, NGC5674) galaxies. The strongest BeppoSAX detections of Sey (such as NGC4151 and IC4329A) were excluded so that single sources would not significantly bias our results. We also excluded from our Sey 2 samples sources with column density in excess of 10^{23} atoms cm^{-2} in order to maintain a certain homogeneity in the absorption properties. The count spectra of the individual observations were added with weights corresponding to the length of time of each observation and the sum was simply normalized by the total number of sources in each subset. Only MECS (3-10 keV) and PDS

data (15-200 keV) were considered in order to avoid the complexity due to the soft excess particularly in Sey 2. Standard data reduction was performed using the software package "SAXDAS" (see <http://www.sdc.asi.it/software> and the Cookbook for BeppoSAX NFI spectral analysis, Fiore, Guainazzi & Grandi 1998). Data were linearized and cleaned for Earth occultation periods and periods of high particle background (satellite passages through the South Atlantic Anomaly). Data have been accumulated for Earth elevation angles > 5 degrees and magnetic cut-off rigidity > 6 . For the PDS data we adopted a fine energy and temperature dependent Rise Time selection, which decreases the PDS background by $\sim 40\%$. This improves the signal to noise ratio of faint sources by about 1.5 (Frontera et al. 1997, Fiore, Guainazzi & Grandi 1998). Data from the four PDS units and the two MECS units were merged after equalization and single MECS and PDS spectra were then accumulated. The normalization constant, introduced to allow for a well known difference in the absolute cross-calibration between the two detectors, was left free to vary between 0.7 -0.95 (Fiore, Guainazzi and Grandi, 1998). All quoted errors refer to 90% confidence level for 1 interesting parameter ($\Delta\chi^2=2.7$). First we fitted the 3-200 keV spectra with an absorbed power law plus a gaussian line (model 1 in table 1). As expected, this simple model provides an unsatisfactory fit to the data mainly due to the presence of a strong reflection component and the possible presence of a high energy cut-off. The iron line energy is compatible with reflection in cold material and the equivalent width (EW) is ~ 100 -200 eV. In both classes of objects the line width is slightly broad but this is likely due to a redshift effect as sources with different z are summed together: in particular 5 Seyfert 1s and 3 Seyfert 2s galaxies have redshift greater than 0.01 which is enough to produce a broadening of the line; an important contribution to the line width could also be given by Fairall 9 ($z=0.047$) to the Sey 1 average spectrum and by NGC5506 ($z=0.062$) to the Seyfert 2s average spectrum. A detailed analysis of the iron line is however beyond the scope of the present paper and it is therefore postponed to a later work.

Although the absorbed power law model points to an overall shape similar for both types of galaxies, the best fit photon index for Sey 1 and 2 turns out to be significantly different: the Sey 1s retain the canonical Γ of ~ 1.9 while the Sey 2s are flatter with $\Gamma \sim 1.75$. As expected Sey 2 galaxies are more absorbed than Sey 1 with an average column density of $\sim 4 \times 10^{22}$ atoms cm^{-2} , however some amount of absorption is also present in Sey 1 galaxies with $N_H \simeq 10^{22}$ atoms cm^{-2} . A recent analysis of a sample of Sey 1 with BeppoSAX indicates that cold absorption of this amount is generally not present in this type of object ($N_H \leq 10^{21}$ atoms cm^{-2}); however a warm absorber seems to be a common feature of type 1 objects and is consistent with the presence of some absorption in our average spectrum (Perola et al. 2002). Next we introduced a Compton reflection component and a high energy cut-off via the pexrav model in XSPEC: this model provides an improvement in the fit which is significant at the 99.99% confidence level for 2 extra degrees of freedom for both classes (table 1

model 2). The inclination assumed for the Seyfert 1s is $\cos i=0.45$ in model 2^a and 0.87 in model 2^b; on the other hand since the Sey 2s are most likely to be seen edge-on, we assumed in this case $\cos i=0.45$ only. Furthermore, we assume the reflection medium to be close to neutral and the abundances used are those of Anders and Ebihara (1982). It is evident from table 1 that while the amount of reflection is consistent between the two types, the primary continuum is still significantly different: the average Sey2 spectrum is substantially harder than that of Sey 1 and the cut-off is at lower energies (see table 1). On the other hand, the average spectrum of Sey 1s is perfectly canonical having $\Gamma=1.9$, a reflection strength $R \sim 0.6$ (or 1 depending on the inclination angle assumed) and a cut-off energy at around 200 keV; the iron line is confirmed at 6.4 keV and the equivalent width is 100-120 keV. Our results confirm the findings of Perola et al. (2002) on a sample of Seyfert 1 galaxies observed by BeppoSAX and analyzed individually with the same model. When their data are combined to get weighted mean values ($\Gamma=1.84 \pm 0.02$, $R=0.64 \pm 0.09$ for $\cos\Theta=0.9$ and $E_{\text{cut}}=130 \pm 20$ keV), these are very similar to our best fit parameters of model 2^b in table 1; their average line energy is at 6.44 ± 0.04 keV while the equivalent width is 122 ± 16 again in agreement with our results. Also, if the iron line comes from the same medium as the Compton reflecting continuum, one would expect a simple relationship between R , Γ and EW, which for the average photon index of the Sey 1 and the reflection value obtained for $\cos\Theta=0.87$ provides an EW value very similar to that observed (see George and Fabian 1991 results rescaled to the Anders and Grevesse (1993) abundances): therefore the observed EW is of the magnitude expected from the simultaneously measured strength of the reflection component. The difference seen between Sey 1 and 2 is however troublesome as it is not easily reconciled with the unified theory, which is however independently supported by other observational evidences.

It is well known that there is an inter-dependence of the parameters in the pexrav model, whereby increasing the reflection and/or the high energy cut-off leads to a steeper power law. To test this possibility, we have imposed a photon index of 1.9 (equal to that obtained for the Sey 1 in the $\cos i=0.45$ configuration) on the Sey 2 and measured the contours of reflection strength against cut-off energy for this case: figure 1 shows the results compared to the Sey 1 case while model 2^{a,c} in table 1 provides the best fit parameters. The cut-off energy turns out to be similar to that measured in type 1 objects but R is now much higher (~ 3). A Compton reflection component as strong as this is unusual for Compton thin Sey 2 galaxies (Bassani et al. 1999) which characterize our sample. Also, following the same reasoning as for type 1 objects, the measured iron line EW is too low for the observed reflection strength especially if a contribution of the order of 30-40 eV has to be taken into account for the line component originating by transmission through a torus of column density of $\sim 4 \times 10^{22}$ cm⁻². A reflection component as strong as that measured is, however, still possible if the hard X-ray emission is isotropic and/or there is a time lag in the response of the reflection

flux to variations of the source intensity (Cappi et al. 1996, Weaver et al. 1996).

A model independent way to verify the presence of a stronger reflection in type 2 with respect to type 1 objects is to measure the Sey 2 to Sey 1 PDS ratio and search for the presence of a bump in the PDS data. The Sey2 to Sey1 ratio is shown in figure 2, which clearly excludes the presence of stronger reflection in type 2 objects. Indeed the average spectra of Sey 1s and Sey 2s appear to be very similar in the high energy (PDS) band, but they are different in the MECS range where effect of absorption takes place.

The ratio shown in figure 2 was produced by first summing the background-subtracted data for the two types of sources individually, normalizing each for the number of sources in each sample and then dividing in order to obtain the ratio. The data were then rebinned in order to have a minimum (3 sigma) detection in each energy bin throughout the ratio. A visual inspection of the distribution of spectra for each sample (figures 3) confirms that neither the Sey 1 or Sey 2 groups are dominated by one source. The origin of the negative counts which can be seen in the individual spectra is due to the fact that we are working in a high energy regime where we are background dominated and statistical variations in background can be higher than the source flux itself. This is confirmed by the observation that the maximum negative flux corresponds to a significance of only 1.5σ , thus ruling out the possibility that systematics in the background subtraction are responsible. The Sey 1 sample is much more homogeneous than the Sey 2 group, which would be expected due to the wider range of geometric orientations possible for the latter type. It can be seen that there is no discernible excess in the 20-100 keV band, thus excluding the presence of stronger reflection in Sey 2's than in Sey 1's; if we restrict the analysis to the 40-70 keV band where excess counts are visible by eye, the significance is still too low (2.3σ) to claim the presence of an excess.

Having excluded reflection as the possible cause of a flatter spectrum, the only other remaining way to steepen the Sey 2 spectrum is via a more complex absorption than assumed. This is not an unreasonable assumption since within our sample there are objects with different column densities and summing their spectra together can artificially produce a complex absorption where the covering fraction depends on the distribution of fluxes. We have therefore introduced in the Sey 2 fit an extra absorber that partially covers the source (model 3^a in Table 1). The fit improves significantly at more than 99% confidence level for two extra degrees of freedom and provides average spectral parameters for the intrinsic continuum very similar to those measured in Sey 1s: $\Gamma \sim 1.9$, $R \sim 0.7-1.2$ and $E_c \sim 200$ keV. The two best fits give rise to two different MECS/PDS normalization factors (~ 0.75 and ~ 0.83) both of which are within the range indicated in the Cookbook of BeppoSAX NFI spectral analysis (Fiore et al. 1998). However, in order to further check the robustness of these results, we have tried to re-analyse the Sey 2 data using the normalization found for the Sey 1's and vice versa. In both cases the values of Γ , R and cut-off are consistent with those found in the original analysis within 2σ . The composite spectra of both types of Seyferts are compared

in figure 4; again from this figure is evident that the two spectra are very similar in the PDS energy range, while differing considerable at lower energies.

3. Conclusions

We have measured with BeppoSAX the average spectra of Sey 1 galaxies confirming previous indications that typically these galaxies have a power law shape with photon index $\Gamma \sim 1.9$, a reflection component of strength $R \sim 0.6-1$ and a high energy cut-off which is now more clearly defined and located at around 200 keV. Sey 2s on the other hand, have an average spectrum which is substantially harder and with a lower energy cut-off than Sey 1s. Our analysis excludes the possibility that stronger reflection in Sey 2s is responsible for their harder spectrum; instead the introduction of a complex absorber provides an average Sey 2's spectrum very similar to that of Sey 1's. This complex absorption is not necessarily intrinsic to individual sources but is likely to be an artifact of summing spectra with different amounts of absorption. However since complex absorption has been observed in some individual source spectra (e.g. Malaguti et al. 1999, Turner et al. 2000) we cannot exclude a-priori its possible contribution to the average Seyfert 2's spectrum. In any case our result on the primary power law continuum argues strongly for a very similar production mechanism not only in both types of Seyferts but in each individual object and is therefore also relevant for the synthesis of the X-ray background: Sey 2 spectra can now be taken to be similar to their type 1 counterparts in the AGN contribution estimates.

We are grateful to M. Cappi for useful discussions. A.M. acknowledge financial support from ASI.

REFERENCES

Anders, E., Ebihara, M. 1982, *Geochim. Cosmochim. Acta* 46, 2363
Anders, E., Grevesse, N. 1993, *Geochim. Cosmochim. Acta* 53, 197
Bassani L., Cappi M., Malaguti G., Palumbo G.G.C., Dadina M. et al. 1999, *Mem S.A.It* Vol.70-1, 65
Cappi M., Mihari T., Matsuoka M., Hayashida K., Weaver K.A., and Otani C. 1996, *ApJ* 458, 149
Fiore F., Guainazzi M., Grandi P. 1998, *BeppoSAX Cookbook*

Frontera F., Costa E., Dal Fiume D., et al. 1997 A&AS, 122, 357

George, I. M. and Fabian, A. C. 1991, MNRASS 249, 352

Malaguti, G., Bassani, L., Cappi, M., Comastri, A., Di Cocco, G., Fabian, A. C., et al. 1999, A&A342L, 41

Matt, G. , Fabian, A. C., Guainazzi, M., Iwasawa, K., Bassani, L., Malaguti, G. 2000, MNRAS, 318, 173

Matt, G. 2001, X-Ray Astronomy, AIP Conference Proceedings edited by N.E. White et al., Vol. 599, p. 209

Perola, G. C., Matt, G., Cappi, M., Fiore, F., et al. 2002, 389, 802

Pounds, K.A. and Reeves, J.N. 2002, astro-ph/0201436, Proceedings of the Symposium on ‘New Visions of the X-ray Universe in the XMM-Newton and Chandra Era’, ESTEC, The Netherlands

Turner, T. J., Perola, G. C., Fiore, F., Matt, G., George, I. M., Piro, L., Bassani, L. 2000, ApJ, 531, 245

Weaver K.A., Nousek J., Yaqoob T., Mushotzky R.F., Makino F., and Otani C. 1996, ApJ 458, 160

Zdziarski, A., Johnson, W. N., Done, C., Smith D., McNaron-Brown K. 1995, ApJ, 438L, 63

Zdziarski, A., Poutanen, J., Johnson, W. N. 2000, ApJ, 542, 703

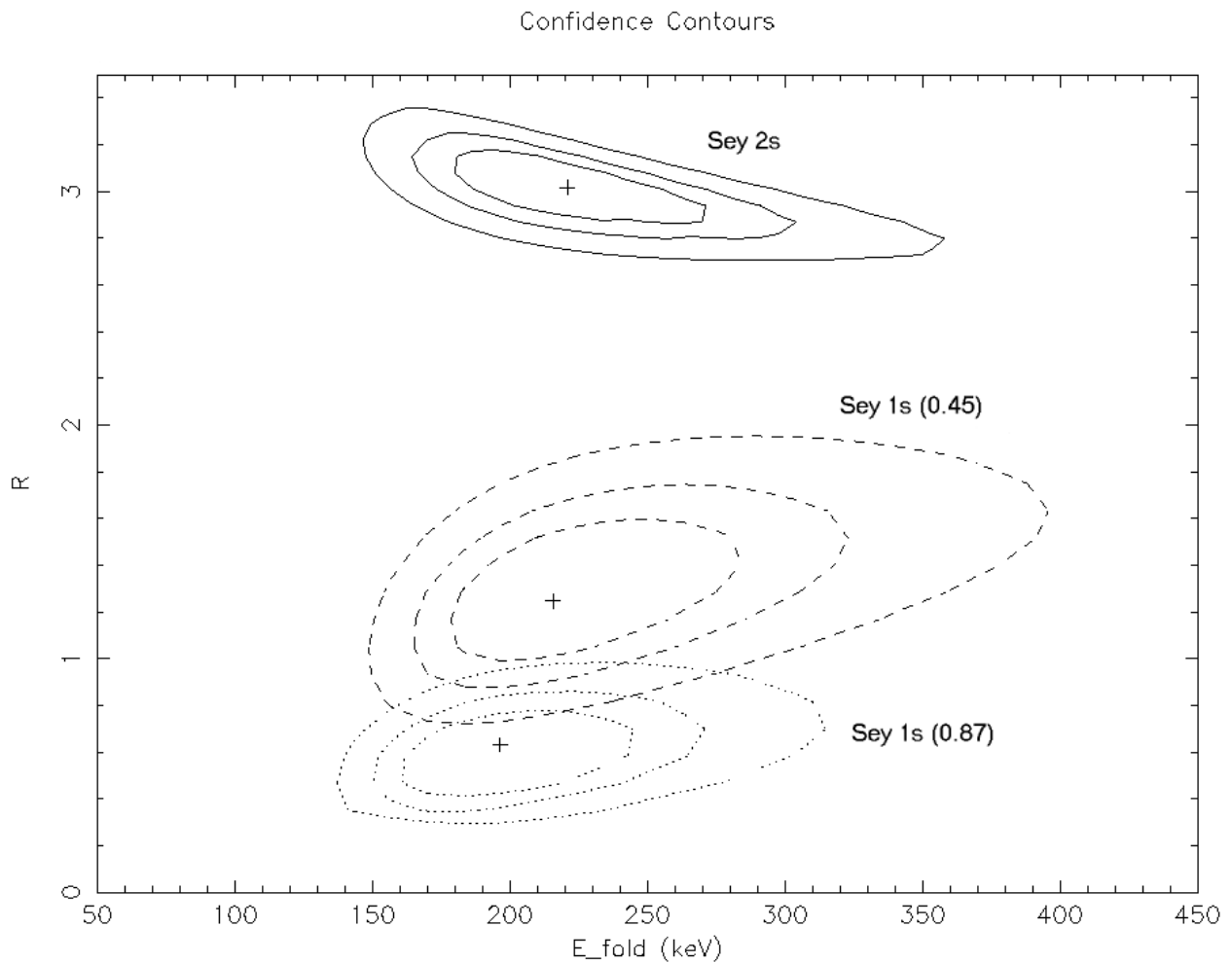


Fig. 1.— Contour plot of reflection versus cut-off with the photon index fixed to 1.9 in the Sey 2 fit.

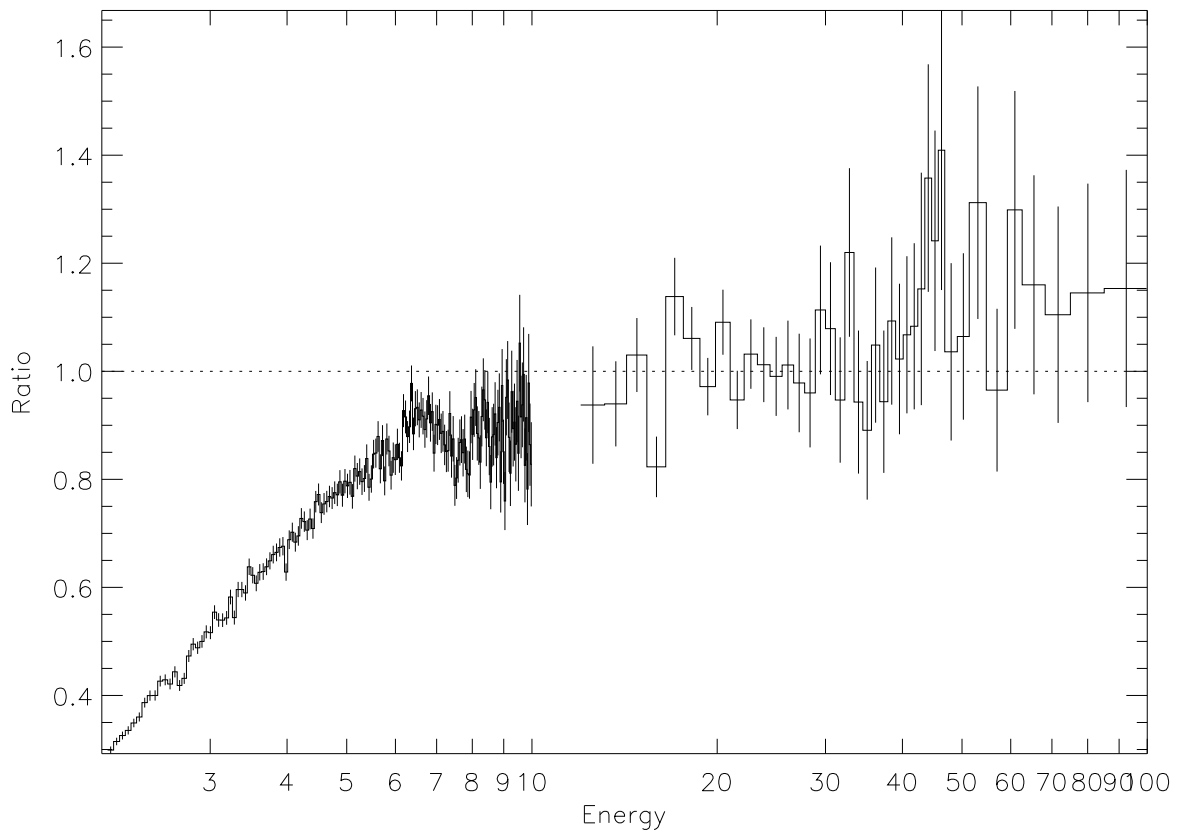


Fig. 2.— The MECS-PDS ratio (Sey2/Sey 1) of the average normalized spectra.

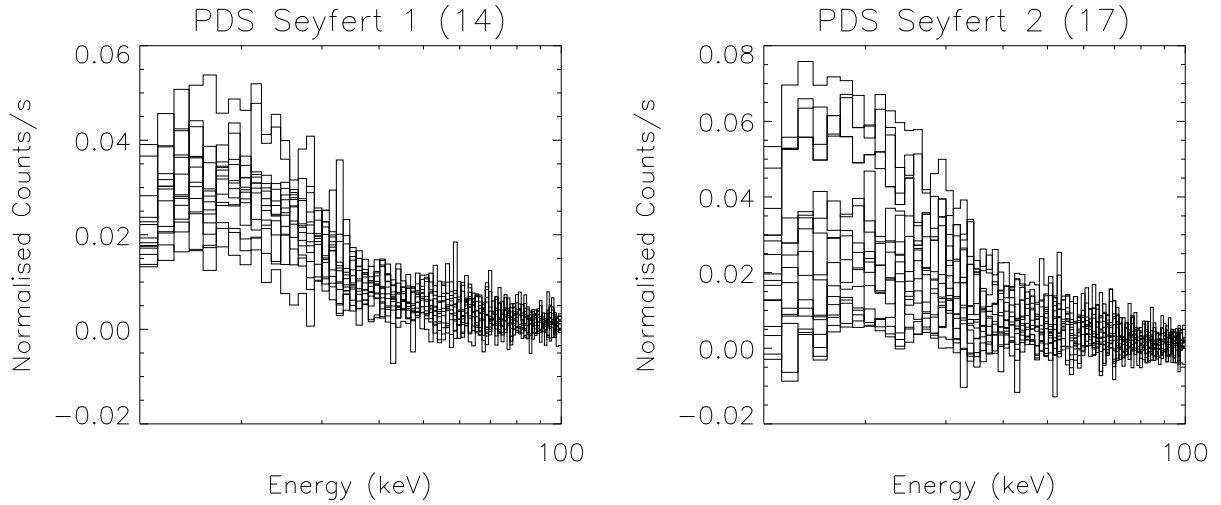


Fig. 3.— The normalized spectra of Sey 1 sample in the PDS detector (left). The normalized spectra of Sey 2 sample in the PDS detector (right). The negative counts present in each set of data are due to the fact that we are working in a high energy regime where we are background dominated and statistical variations in background can be higher than the source flux itself.

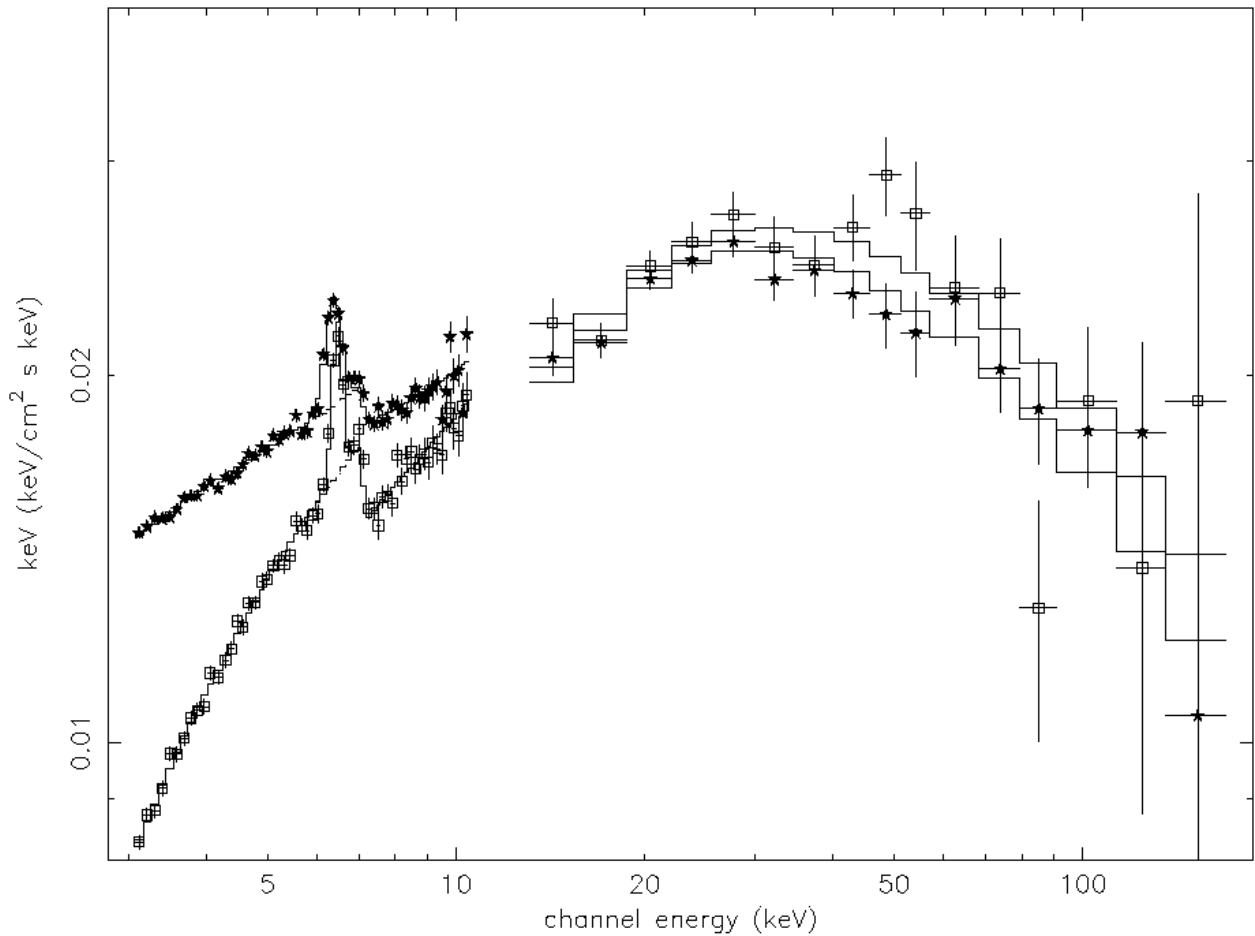


Fig. 4.— Comparison of the unfolded spectra of Sey 1s (stars) fitted with pexrav model and Sey 2s (squares) fitted with double absorption plus pexrav model

Table 1.

Parameter	Seyfert 1s			Seyfert 2s			
	Model 1	Model 2 ^a	Model 2 ^b	Model 1	Model 2 ^a	Model 2 ^{a,c}	Model 3 ^a
$N_H(1) \times 10^{22}$	$1.01^{+0.15}_{-0.17}$	$0.93^{+0.18}_{-0.18}$	$0.87^{+0.18}_{-0.19}$	$4.12^{+0.23}_{-0.22}$	$3.67^{+0.29}_{-0.27}$	$3.83^{+0.24}_{-0.30}$	$3.16^{+0.50}_{-0.13}$
$N_H(2) \times 10^{22}$	27^{+5}_{-4}
C_f	$0.26^{+0.04}_{-0.03}$
Photon Index	$1.85^{+0.01}_{-0.02}$	$1.92^{+0.04}_{-0.03}$	$1.88^{+0.04}_{-0.03}$	$1.74^{+0.02}_{-0.02}$	$1.75^{+0.06}_{-0.04}$	1.90	$1.89^{+0.02}_{-0.13}$
E_{fold}	...	216^{+75}_{-41}	197^{+64}_{-40}	...	128^{+45}_{-24}	221^{+94}_{-61}	226^{+69}_{-48}
R	...	$1.25^{+0.38}_{-0.29}$	$0.64^{+0.22}_{-0.19}$...	$1.19^{+0.64}_{-0.35}$	$3.02^{+0.28}_{-0.27}$	$0.96^{+0.29}_{-0.24}$
E_{line} (keV)	$6.39^{+0.04}_{-0.04}$	$6.37^{+0.03}_{-0.03}$	$6.38^{+0.04}_{-0.04}$	$6.48^{+0.06}_{-0.10}$	$6.47^{+0.03}_{-0.04}$	$6.44^{+0.04}_{-0.03}$	$6.46^{+0.03}_{-0.03}$
σ_{line} (keV)	$0.26^{+0.06}_{-0.05}$	$0.18^{+0.03}_{-0.14}$	$0.22^{+0.06}_{-0.08}$	$0.25^{+0.07}_{-0.02}$	$0.21^{+0.06}_{-0.11}$	$0.10^{+0.06}_{-0.10}$	$0.12^{+0.07}_{-0.12}$
EW (eV)	148^{+19}_{-18}	106^{+18}_{-29}	120^{+21}_{-20}	189^{+26}_{-25}	145^{+71}_{-36}	97^{+17}_{-14}	103^{+13}_{-19}
χ^2/dof	257.41 (70)	87.12 (68)	90.48 (68)	242.62 (70)	101.92 (68)	108.54 (69)	90.4 (66)
χ^2_ν	3.68	1.25	1.33	3.47	1.50	1.57	1.37
	,,						

^a $\cos\Theta=0.45$ (fixed)

^b $\cos\Theta=0.87$ (fixed)

^c $\Gamma=1.90$ (fixed)

Note. — **Model 1** = wa*po+ga (absorbed power law + gaussian line); **Model 2** = wa*(pexrav+ga) (absorbed exponentially cut off power law spectrum reflected from neutral material); **Model 3** = wa*pcfabs*(pexrav+ga) (as Model 2 plus a partial covering fraction absorption).